Journal of Photochemistry and Photobiology A: Chemistry 217 (2011) 1–9

Contents lists available at ScienceDirect

Journal of Photochemistry and Photobiology A: Chemistry

journal homepage: www.elsevier.com/locate/jphotochem

Structure and sensitized near-infrared luminescence of Yb(III) complexes with sulfonylamidophosphate type ligand

Paula Gawryszewska[a,*], Olesia V. Moroz[b], Victor A. Trush[b], Dagmara Kulesza[a], Vladimir M. Amirkhanov[b]

[a] Faculty of Chemistry, University of Wroclaw, 14 F. Joliot-Curie St., 50-383 Wroclaw, Poland
[b] Department of Chemistry, Kyiv National Taras Shevchenko University, Volodymyrska St. 64, Kyiv 01601, Ukraine

ARTICLE INFO

Article history:
Received 19 March 2010
Received in revised form 15 June 2010
Accepted 29 June 2010
Available online 7 July 2010

Keywords:
Sulfonyl phosphoramides
Ytterbium chelates
Near-infrared luminescence
Energy transfer
Crystal structure

ABSTRACT

A series of new lanthanide complexes with dimethyl(phenylsulfonyl)amidophosphate (H**SP**) was synthesized ($\{Na[Ln(SP)_4]\}_n$ (**Ln1**), $[Ln(SP)_3phen]$ (**Ln2**) and $[Ln(SP)_3bpy]\cdot H_2O$ (**Ln3**) (where Ln = Gd^{III}, Er^{III}, Yb^{III} and Lu^{III}; phen = 1,10-phenantroline; and bpy = 2,2′-bipyridine) and the crystal structures of $[Er(SP)_3phen]$ and $[Yb(SP)_3bpy]\cdot H_2O$ were resolved. Absorption (at 295, 4 K), emission (at 295, 77, 4 K) and IR (at 295 K) spectra as well as luminescence decay time measurements were used to characterize the photophysical properties of single crystals. Effective energy transfer from a **[SP]**$^-$ ligand to the Yb^{III} ion was demonstrated despite a large energy gap $\Delta E = E_{trip} - E_{^2F_{5/2}}$. Replacing one molecule of the **[SP]**$^-$ ligand with the phen or bpy molecule caused reduction of the emission decay time from 35 μs for **Yb1** to 20 and 15.5 μs for **Yb2** and **Yb3**, respectively at the temperature of 295 K. Using the absorption spectra τ_{rad} (1.1 ms—**Yb1**, 943 μs—**Yb2** and 914 μs—**Yb3**) and Q_{Ln}^{Ln} (3.14%—**Yb1**, 2.19%—**Yb2**, 1.64%—**Yb3**) were estimated. On the basis of low temperature, high-resolution absorption and luminescence spectra, the ligand-field splittings of the excited and ground states of Yb^{III} complexes were determined.

1. Introduction

Photophysical properties of lanthanide ions have attracted a lot of attention in the past few decades. The intense, long luminescent lifetimes in the micro-millisecond range, line-like emission of phosphorescent ions such as Sm^{III}, Eu^{III}, and Tb^{III} in the visible region are used in the lighting industry [1], optical fibres for telecommunications [2,3], their capacity in forming functional complexes for biological assays [4] and medical imaging purposes [5]. On the other hand, in the recent years there has been an increasing interest in the photophysical properties of complexes with lanthanide ions such as Yb^{III}, Nd^{III}, Pr^{III} and Er^{III}, which are luminescent in NIR region. The interest in near-infrared luminescent materials results from the possibility of their usage in telecommunications and laser design [6], for instance, the presence of Cotton effect displayed by the $^2F_{5/2} \leftarrow {}^2F_{7/2}$ transition of Yb^{III}-containing compounds has been used in the study of antibiotics [7], a NIR-emissive protein conjugate has been applied as luminescent label in clinic diagnostics [8–10]. The extensiveness of the investigations on NIR sensitized luminescence makes it impossible that even majority of the papers are cited, especially as they can be found in the recently published reviews. Two of them are included as Ref. [11]. Most of the papers deal with complexes in non-aqueous solutions [11–14], some of them in aqueous solutions [11–21] or in the solid state [11,17,22]. The lanthanide ion, frequently investigated especially in inorganic materials [23–25], as well as recently in molecular devices, is the Yb^{III} ion. Yb^{III} possesses only one excited state ($^2F_{5/2}$) around 1 μm, with the rest of the NIR and VIS spectrum transparent. This is an interesting ion, not only due to its applications, but also because of the ligand-to-metal energy transfer mechanism, especially where the energy gap between ligand triplet state and excited level of Yb^{III} is very large, about 15,000 cm^{-1}. For systems where there is a poor overlap between the triplet state and the Yb^{III} excited state, Horrocks et al. [26] have suggested that a sensitized Yb^{III} luminescence occurs via a long range electron transfer process. Reinhard and Güdel [17] have proposed a single-configurational coordinate model to rationalize the non-radiative relaxation step from the ligand-centered to the metal-centered excited state. Even though fundamentals of non-radiative energy transfer involving lanthanide ions are well established [27–29] there are several aspects not yet firmly understood. Recently, theoretical background of the Coulomb direct and exchange interactions in non-radiative energy transfer involving lanthanide ions was critically reviewed [30].

In order to overcome a very small absorption coefficient of the f–f transitions excitation usually relies on energy transfer from the

* Corresponding author. Tel.: +48 71 375 73 94; fax: +48 71 375 74 20.
E-mail address: paula@wchuwr.pl (P. Gawryszewska).

1010-6030/$ – see front matter © 2010 Elsevier B.V. All rights reserved.
doi:10.1016/j.jphotochem.2010.06.033

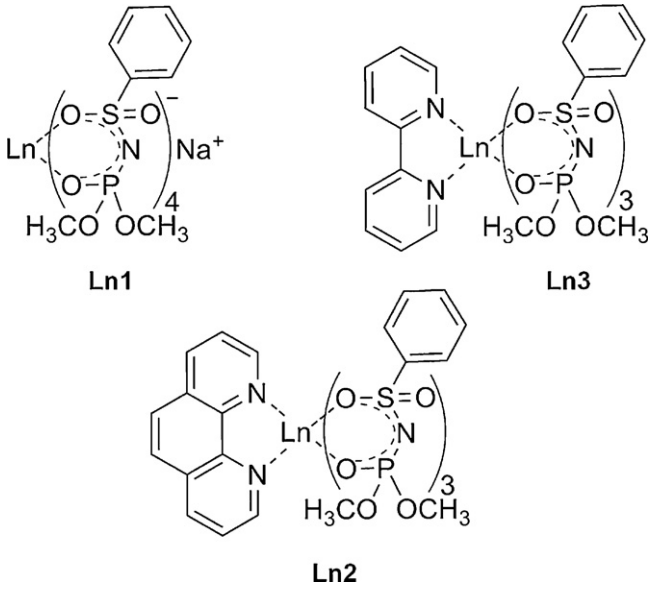

Scheme 1. New complexes described in this paper.

surrounding ligands to the lanthanide ion. The rare earth coordination chemistry has been widely characterized by complexes with a large class of π-conjugated ligands such as β-diketones, the ligands were proved to be exceptional antenna ligands forming facile complexes with Ln^{III} ions [27a,28,31–34]. In the previous work [35], we presented a synthesis and full characteristic of a sulfonyl phosphoramide derivative—dimethyl(phenylsulfonyl)amidophosphate (H**SP**) of the general formula $C_6H_5SO_2NHP(O)(OCH_3)_2$. This type of phosphoramides with different substituents at sulfur and phosphorus atoms was first synthesized by Kirsanov [36].

It was earlier described that dimethyl(phenylsulfonyl)amidophosphate anions can form $[Ln(\mathbf{SP})_4]^-$-type complexes, the crystal structure of the $\{Na[Nd(SP)_4]\}_n$ has been reported [37]. It is important that in $[Ln(\mathbf{SP})_4]^-$ lanthanide ions form thermodynamically stable highly coordinated complexes without the possibility of solvent molecules coordination. 1,10-Phenantroline (phen) or 2,2′-bipyridine (bpy) has been widely used as additional ligands for some lanthanide complexes with β-diketonates to replace water molecules [27a,34].

In this paper, we describe the syntheses, crystal structures and photophysical properties of a new series of NIR emitting lanthanide complexes (Scheme 1). Complexes with ligands of sulfonylamidophosphate type besides very interesting luminescence properties constitute a new partition of coordination chemistry of those ligands.

2. Experimental part

2.1. Compounds synthesis

2.1.1. Na[Ln(SP)$_4$]

Methanol solution of sodium methylate, prepared by dissolving sodium (0.092 g, 4 mmol), was added to 30 ml of a stirred solution of H**SP** (1.060 g, 4 mmol) in MeOH. The resulting solution was evaporated to obtain a pale yellow powder of Na**SP**. It was purified by recrystallization from isopropanol solution. $Ln(NO_3)_3{\cdot}nH_2O$ (1 mmol) was dissolved in acetone (20 ml) and added to 50 ml of acetone solution of Na**SP** (1.149 g, 4 mmol). After 20 min the precipitate of $NaNO_3$ was filtered off and 10 ml of isopropanol was added to the filtrate. The resulting clear solution was left at ambient temperature for crystallization in air. The crystals suitable for single X-ray analysis were separated by filtration after 48 h, washed with cold isopropanol and air-dried. The complexes are stable in air, soluble in polar organic solvents and hot water.

Na[Gd(SP)$_4$]: yield: 1.05 g (0.85 mmol, 85%). Anal. Calcd for $C_{32}H_{44}N_4O_{20}P_4S_4NaGd$ (MW 1237.09): C, 31.07; H, 3.58; N, 4.53; S, 10.37%. Found: C, 31.01; H, 3.33; N, 4.42; S, 10.23%. IR ν_{max}: 1390, 1250, 1180, 1135, 1055, 855, 570 cm^{-1}.

Na[Er(SP)$_4$]: yield: 1.00 g (0.80 mmol, 80%). Anal. Calcd for $C_{32}H_{44}N_4O_{20}P_4S_4NaEr$ (MW 1247.10): C, 30.82; H, 3.56; N, 4.49; S, 10.28%. Found: C, 30.72; H, 3.51; N, 4.56; S, 10.20%. IR ν_{max}: 1390, 1250, 1180, 1135, 1055, 855, 570 cm^{-1}.

Na[Yb(SP)$_4$]: yield: 0.99 g (0.79 mmol, 79%). Anal. Calcd for $C_{32}H_{44}N_4O_{20}P_4S_4NaYb$ (MW 1252.97): C, 30.65; H, 3.54; N, 4.47; S, 10.21%. Found: C, 30.43; H, 3.67; N, 4.58; S, 10.12%. IR ν_{max}: 1390, 1250, 1180, 1135, 1055, 855, 570 cm^{-1}.

Na[Lu(SP)$_4$]: yield: 1.03 g (0.82 mmol, 82%). Anal. Calcd for $C_{32}H_{44}N_4O_{20}P_4S_4NaLu$ (MW 1254.81): C, 30.63; H, 3.53; N, 4.46; S, 10.22%. Found: C, 29.98; H, 3.59; N, 4.45; S, 10.07%. IR ν_{max}: 1390, 1250, 1180, 1135, 1055, 855, 570 cm^{-1}.

2.1.2. [Ln(SP)$_3$bpy]·H$_2$O

To an acetone solution (10 ml) of Na**SP** (0.862 g, 3 mmol), the acetone solution of $Ln(NO_3)_3{\cdot}nH_2O$ (5 ml) (1 mmol) was added, and the mixture was stirred for 15 min. The precipitate of $NaNO_3$ was filtered off and isopropanol solution of bpy (0.156 g, 1 mmol) was added dropwise. The resulting clear solution was left for slow evaporation at ambient temperature. The well-shaped crystals, formed within 3 days, were isolated by filtration, washed with cold isopropanol and air-dried. The complexes are stable in air, soluble in polar organic solvents and hot water.

[Er(SP)$_3$bpy]·H$_2$O: yield: 1.02 g (0.90 mmol, 90%). Anal. Calcd for $C_{34}H_{43}N_5O_{16}P_3S_3Er$ (MW 1134.10): C, 36.01; H, 3.82; N, 6.18; S, 8.48%. Found: C, 35.79; H, 3.68; N, 6.26; S, 8.68%. IR ν_{max}: 1265, 1210, 1175, 1050, 565 cm^{-1}.

[Yb(SP)$_3$bpy]·H$_2$O: yield: 0.91 g (0.81 mmol, 81%). Anal. Calcd for $C_{34}H_{43}N_5O_{16}P_3S_3Yb$ (MW 1139.88): C, 35.83; H, 3.80; N, 6.14; S, 8.44%. Found: C, 36.17; H, 3.95; N, 6.19; S, 8.32%. IR ν_{max}: 1265, 1210, 1175, 1050, 565 cm^{-1}.

[Lu(SP)$_3$bpy]·H$_2$O: yield: 0.98 g (0.87 mmol, 87%). Anal. Calcd for $C_{34}H_{43}N_5O_{15}P_3S_3Lu$ (MW 1141.81): C, 35.77; H, 3.80; N, 6.13; S, 8.42%. Found: C, 34.90; H, 3.81; N, 6.34; S, 8.22%. IR ν_{max}: 1270, 1210, 1180, 1050, 570 cm^{-1}.

2.1.3. [Ln(SP)$_3$phen]

Crystals of [Ln(SP)$_3$phen] were isolated with the use of phen as an additional ligand and following exactly the same procedure as described above for the corresponding [Ln(SP)$_3$bpy]·H$_2$O complexes. The complexes are stable in air, soluble in polar organic solvents and hot water.

[Gd(SP)$_3$phen]: yield: 0.94 g (0.83 mmol, 83%). Anal. Calcd for $C_{36}H_{41}N_5O_{15}P_3S_3Gd$ (MW 1130.10): C, 37.96; H, 3.63; N, 6.15; S, 8.43%. Found: C, 37.90; H, 3.67; N, 6.19; S, 8.40%. IR ν_{max}: 1260, 1175, 1045, 860, 560 cm^{-1}.

[Er(SP)$_3$phen]: yield: 1.04 g (0.91 mmol, 91%). Anal. Calcd for $C_{36}H_{41}N_5O_{15}P_3S_3Er$ (MW 1138.03): C, 37.96; H, 3.63; N, 6.15; S, 8.43%. Found: C, 37.90; H, 3.66; N, 6.17; S, 8.40%. IR ν_{max}: 1260, 1175, 1045, 860, 560 cm^{-1}.

[Yb(SP)$_3$phen]: yield: 0.97 g (0.85 mmol, 85%). Anal. Calcd for $C_{36}H_{41}N_5O_{15}P_3S_3Yb$ (MW 1146.04): C, 37.73; H, 3.61; N, 6.11; S, 8.39%. Found: C, 37.77; H, 3.63; N, 6.10; S, 8.42%. IR ν_{max}: 1265, 1180, 1055, 860, 565 cm^{-1}.

[Lu(SP)$_3$phen]: yield: 1.03 g (0.9 mmol, 90%). Anal. Calcd for $C_{36}H_{41}N_5O_{15}P_3S_3Lu$ (MW 1147.81): C, 37.67; H, 3.60; N, 6.10; S, 8.38%. Found: C, 37.73; H, 3.62; N, 6.12; S, 8.41%. IR ν_{max}: 1270, 1180, 1055, 865, 565 cm^{-1}.

2.2. X-ray measurements

X-ray data for [Er(SP)$_3$phen] (**Er2**) and [Yb(SP)$_3$bpy]·H$_2$O (**Yb3**) were collected at low temperature using an Oxford Cryosystem device on a Kuma KM4CCD κ-axis diffractometer with graphite-monochromated Mo Kα radiation (λ = 0.71073 Å). The crystal was positioned at 65 mm from the CCD camera. 612 frames were measured at 0.75° intervals with a counting time of 20 s. Accurate cell parameters were determined and refined by least-squares fit of 6300 strongest reflections. The data was corrected for Lorentz and polarization effects. Analytical absorption correction was also applied. Data reduction and analysis were carried out with the Oxford Diffraction (Poland) programs. The structure was solved by direct methods (program SHELXS97 [38]) and refined by the full-matrix least-squares method on all F2 data using the SHELXL97 [39] programs. Non-hydrogen atoms were refined with anisotropic displacement parameters; hydrogen atoms from $\Delta\rho$ maps were included. They were refined with isotropic displacement parameters.

Crystallographic data for the structures reported in this paper (excluding structure factors) has been deposited in the Cambridge Crystallographic Data Centre, CCDC No. 753871 for **Yb3** and CCDC No. 753872 for **Er2**. Copies of this information may be obtained free of charge from the Director, CCDC, 12 UNION Road, Cambridge 1EZ. UK (fax: +44-1223-336033; e-mail: deposit@ccdc.cam.ac.uk or http://www.ccdc.cam.ac.uk)

2.3. Spectroscopic measurements

Absorption measurements were performed using a Cary-Varian 500 spectrophotometer.

Emission spectra were measured with a SpectraPro 750 monochromator, equipped with InGaAs detector with a 3 mm element and 600 l/mm grating blazed at 1600 nm. The 450 W xenon arc lamp was used as an excitation source, coupled with 275 mm excitation monochromator using a 1800 l/mm grating blazed at 250 nm. Excitation spectra have been corrected for the excitation light intensity, while emission spectra were not corrected for the instrument response.

Alternatively, the fourth harmonic (266 nm) of Nd:YAG pulsed laser (LASER SYSTEM LS-2137/2 M, LOTISII) and add-on device Ti:Al_2O_3 generating laser radiation of 350–500 nm and 690–1000 nm were applied to excite the samples. In this case the emission spectra were recorded with THR 1000 Jobin-Yvon spectrophotometer equipped with CCD camera and Hammamatsu R406 photomultiplier. The same set-up, combined with Lecroy Wave Surfer 400 Oscilloscope, was used for decay time measurements.

The absorption and luminescence measurements were performed at room, 77 K and 4 K temperatures, using liquid-N_2 cooled quartz dewar or Oxford 1204 helium continuous flow cryostat.

The phosphorescence was excited by 266 nm line of Nd:YAG pulsed laser and the spectra were collected using CCD OceanOptics SD-2000 spectrophotometer, directly after switching off the excitation source.

IR spectra were recorded as Nujol or fluorinated Nujol mull using Bruker IFS66/S FTIR spectrometer in the 4000–50 cm^{-1} region.

Elemental analysis (C, H, N, and S) was performed using EL III Universal CHNOS Elemental Analyzer.

Refractive indexes were determined immersion method.

3. Results and discussion

3.1. X-ray analysis

For complex preparation, the molar ratio between the Ln(NO$_3$)$_3$·nH$_2$O and the β-diketonate investigated was determined to be 1:4 or 1:3 [40]. Herein, similar coordination compounds with 1:4 or 1:3 molar ratio have been synthesized for dimethyl(phenylsulfonyl)amidophosphate (H**SP**). When the ratio is 1:4, the saturated tetrakis-complexes can be obtained with four deprotonated ligands **[SP]**$^-$, coordinated to one lanthanide ion. However, the presence of unsaturated coordination sphere of lanthanide ion in a complex with the molar ratio 1:3 (coordination numbers of lanthanide ions are typically 8 or 9) can be used for obtaining a considerable number of mix-ligand compounds by interaction of Ln(**SP**)$_3$ with various donor agents. In the present work, bpy and phen were used as the additional bidentate chelate ligand. The reaction of Ln(**SP**)$_3$ with an equimolar amount of bpy or phen in acetone/isopropanol solution leads to the formation of complexes with the general formula [Ln(**SP**)$_3$bpy]·H$_2$O or [Ln(**SP**)$_3$phen], respectively. Syntheses of all compounds were conducted out in the air.

3.1.1. {Na[Yb(SP)$_4$]}$_n$ (*Yb1*)

The presented **Yb1** compound is isostructural with {Na[Nd(**SP**)$_4$]}$_n$ (**Nd1**) complex, where lanthanide ion occupies one equivalent position in the structure [41]. The complexes crystallize as a polymer in the monoclinic system with space group $P2_1/c$. The Ln^{III} ion is eight-coordinated by oxygen atoms belonging to the sulfonyl and phosphoryl groups of four bidentate chelate ligands. Oxygen atoms of [**SP**]$^-$ ligands create six-membered chelating rings, where the Ln–O bond lengths to the [**SP**]$^-$ ligands are in the expected range, with the Ln–O(S) distances being about 0.15 Å longer than the Ln–O(P) distances. The shortest bond in **Nd1** is 2.358(2) Å while the longest is 2.540(2) Å, where the oxygen atoms belong to the phosphoryl and sulfonyl groups, respectively. The polymeric connection of complex anions is provided by Na ions, whose coordination number is five due to the bonding with two oxygen atoms from one complex anion and next two oxygen and nitrogen atoms from the neighbour ones. The Ln–Ln distance in polymeric chain equals 11.54 Å.

3.1.2. [Er(SP)$_3$phen] (*Er2*) and [Yb(SP)$_3$bpy]·H$_2$O (*Yb3*)

The presented **Yb2** compound is isostructural with **Er2**. Single-crystal X-ray diffraction studies revealed similar crystal structures for **Er2** and **Yb3** complexes, whose crystals fall in the same centrosymmetric space group – $P\bar{1}$. Both of them crystallize as monomers. The unit cell of dimensions a = 9.585(3) Å, b = 11.981(3) Å, c = 19.696(6) Å, and a = 10.110(5) Å, b = 11.757(6) Å, c = 19.565(9) Å, respectively for **Er2** and **Yb3**, consists of two formula units. The molecular structures, with the numbering scheme for atoms and the elementary cells, are shown in Fig. 1a and b and in Fig. 2a and b, respectively. The crystallographic data of **Er2** and **Yb3** are presented in Table 1.

The Ln^{III} ion is eight-coordinated with the first coordination sphere made up of three deprotonated [**SP**]$^-$ ligands and one phenantroline molecule as the second ligand for **Er2**, or one bipyridine molecule as the second ligand for **Yb3**. One phosphoryl oxygen atom (O52, O53, O54 for **Er2** and **Yb3**), one sulfonyl oxygen atom (O12, O13, O14 for **Er2** and **Yb3**) of each [**SP**]$^-$ ligands in both complexes and two nitrogen atoms (N11, N21 for **Er2** and for **Yb3**) of second ligands are involved in lanthanide-ion coordination. Oxygen atoms of [**SP**]$^-$ ligands, in both types of complexes, create six-membered chelating rings, where the Ln–O bond lengths to the [**SP**]$^-$ ligands are in the expected range, with the Ln–O(S) distances being about 0.1 Å longer than the Ln–O(P) distances. The shortest bond in **Er2** is Er–O(52) (2.258(2) Å), while the longest is Er–O(14) (2.446(2) Å), where the oxygen atoms belong to the phosphoryl and sulfonyl groups, respectively. The shortest bond in **Yb3** is Yb–O(53) (2.230(3) Å), while the longest is Yb–O(14) (2.407(3 Å). For **Er2** and **Yb3** Ln–N(11) and Ln–N(21) bond lengths creating five-membered chelating rings are also in the expected range. Selected bond lengths

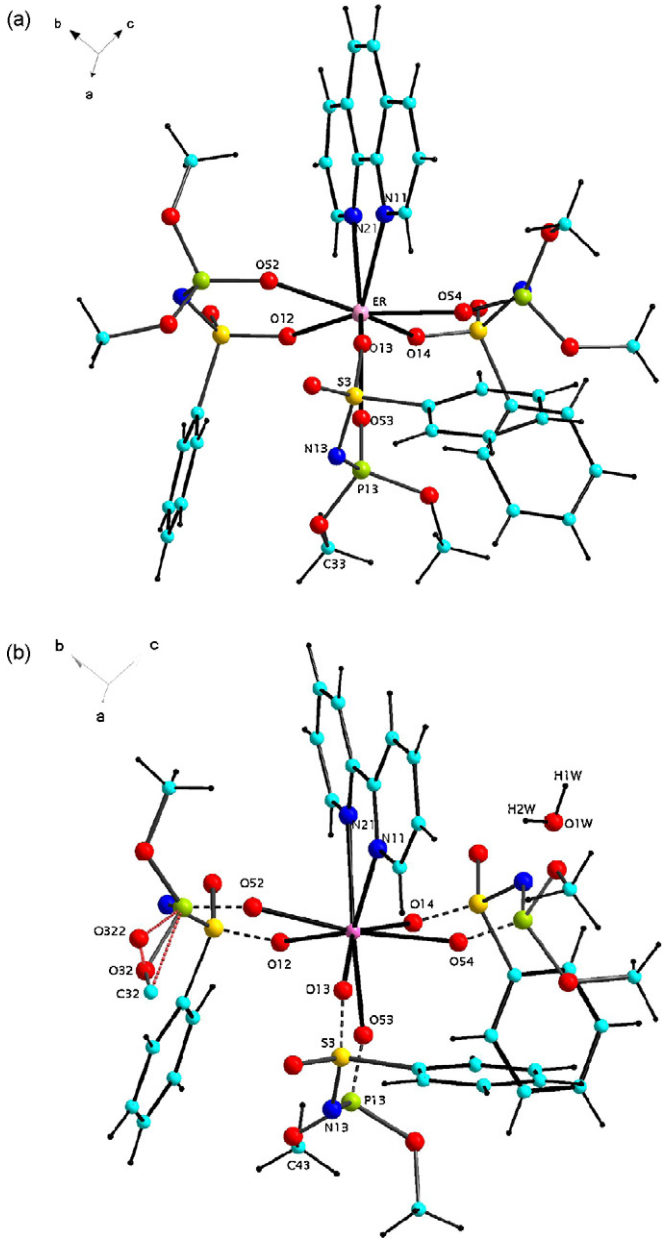

Fig. 1. The X-ray structures of (a) [Er(SP)$_3$phen] and (b) [Yb(SP)$_3$bpy]·H$_2$O.

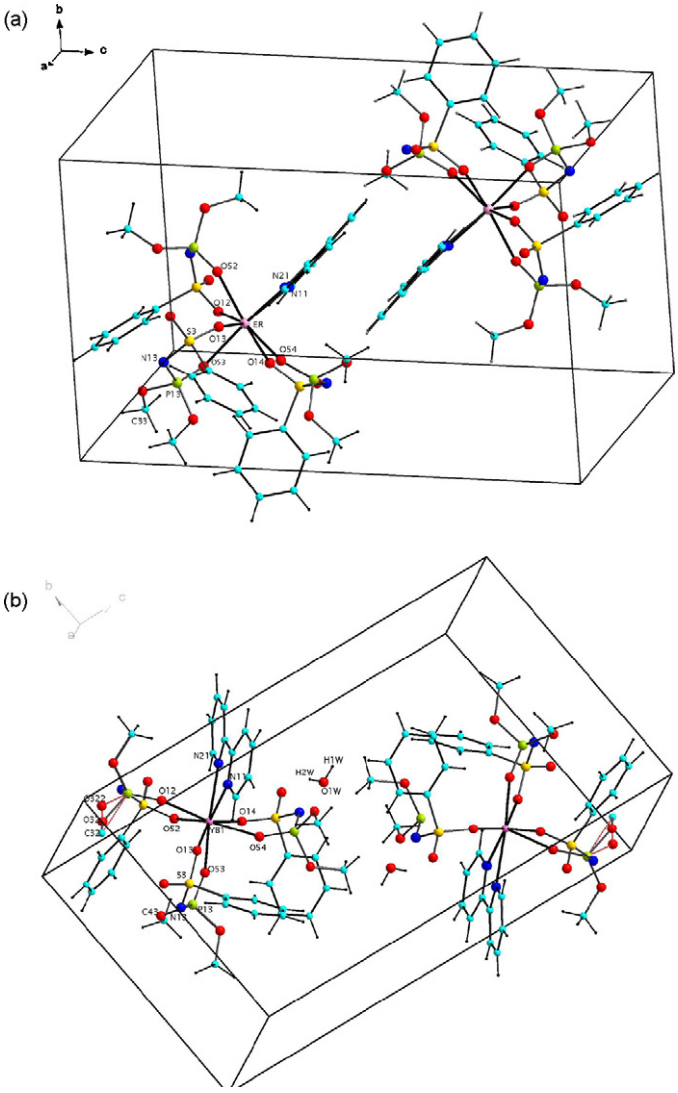

Fig. 2. The elementary cells of (a) [Er(SP)$_3$phen] and (b) [Yb(SP)$_3$bpy]·H$_2$O.

and angles are given in Table 2. The coordination geometry of the metal ion can be described as a distorted square antiprism with six oxygen atoms and two nitrogen atoms. The main difference between structures of **Er2** and **Yb3** is the presence of one water molecule in the second coordination sphere of **Yb3**.

3.2. Spectroscopic results

3.2.1. IR spectroscopy

The vibration of the amide group ν(N–H) in IR spectra of H**SP** appears in the region of 2800–3200 cm^{-1} with the maxima at 3000 cm^{-1}. This band is absent in the spectra of Na**SP** and all complexes **Ln1**, **Ln2** and **Ln3**, which can be due to the fact that ligands exist in coordination compounds in deprotonated forms ([**SP**]$^-$). Two sharp bands, observed in the spectrum of free ligand with maxima at 1260 and 1320 cm^{-1}, are assigned to ν(PO) and ν(SO) vibrations. In the spectra of Na**SP** and obtained complexes, the bands are shifted to lower frequencies (Δ(PO) = 75 cm^{-1} and Δ(SO) = 90 cm^{-1} for Na**SP**, Δ(PO) = 80 cm^{-1} and Δ(SO) = 70 cm^{-1} for **Ln1**, Δ(PO) = 80–85 cm^{-1} and Δ(SO) = 55–60 cm^{-1} for **Ln2** and **Ln3**, which can be explained by coordination to the metal atom. The analysis of IR spectra suggests a bidentate coordination of the ligand in the anionic form [**SP**]$^-$ via the oxygen atoms of phosphoryl and sulfonyl groups.

In the 315–610 cm^{-1} region the ν(Ln–O) stretching motions couple with the chelate ring vibrations appear. The broad and middle intensity bands observed in the 50–290 cm^{-1} region should be described as δ(OLnO) and γ(O–Ln–O) motions (**Yb1**: 93, 115, 172, 211, 243, 256 and 293 cm^{-1}; **Yb2**: 113, 173, 205, 243 and 270 cm^{-1}; **Yb3**: 94, 116, 131, 169, 216, 248, 263 and 296 cm^{-1}).

The most notable feature in the IR spectra of **Yb1** and **Yb2** is the absence of O–H stretching vibrations, which can be an indication of the absence of coordinated water molecules, which is in turn in good agreement with the results of the elemental analysis and single X-ray crystal analyses.

3.2.2. Absorption and luminescence spectroscopy

Room temperature absorption spectra of **Yb1**, **Yb2** and **Yb3** in alcoholic solutions are presented in Fig. 3. The complex with H**SP** ligands (**Yb1**) is stable in CH$_3$OH and displays absorption band with fourth maximums around 260 nm. Molar absorption coefficient (ε) for methanolic solutions of **Yb1** is equal 2565 M^{-1} cm^{-1} (264 nm).

Table 1
Crystal data and structure refinement for [Er(SP)$_3$Phen] (**Er2**) and [Yb(SP)$_3$bpy]·H$_2$O (**Yb3**).

Empirical formula	$C_{36}H_{41}N_5ErO_{15}P_3S_3$	$C_{34}H_{43}N_5O_{16}P_3S_3Yb$
Formula weight	1140.09	1139.86
Temperature (K)	100(2)	100(2)
Wavelength (Å)	0.71073	0.71073
Crystal system	Triclinic	Triclinic
Space group	$P\bar{1}$	$P\bar{1}$
a (Å)	9.585(3)	10.110(5)
b (Å)	11.981(3)	11.757(6)
c (Å)	19.696(6)	19.565(9)
α (°)	93.07(3)	100.34(4)
β (°)	99.76(3)	97.18(4)
γ (°)	101.57(3)	103.79(4)
Volume (Å^3)	2174.8(7)	2187.3(19)
Z	2	2
D_c (Mg m^{-3})	1.681	1.731
Mu (mm^{-1})	2.26	2.46
F(0 0 0)	1068	1146
θ range for data collection (°)	3.08–36.86	2.73–25.07
Ranges of h, k, l	$-15 \le h \le 15$ $-19 \le k \le 19$ $-24 \le l \le 33$	$-11 \le h \le 12$ $-12 \le k \le 14$ $-23 \le l \le 22$
Reflections collected	38,250	16,727
Independent reflections (R_{int})	17,107 (0.0398)	7701 (0.0308)
Parameters	576	564
S	0.996	0.987
Final R_1/wR_2 indices ($I > 2\sigma_I$)	$R_1 = 0.0387$, $wR_2 = 0752$	$R_1 = 0.0302$, $wR_2 = 0.0728$
Largest diff. peak/hole (e Å^{-3})	1.31 and −0.96	0.94 and −0.92

For **Yb2** and **Yb3** additionally phenathroline and bipyridine bands are visible. They are centred at 272 nm (ε = 21,864 M^{-1} cm^{-1}), 293 nm (ε = 9503 M^{-1} cm^{-1}), 327 nm (ε = 661 M^{-1} cm^{-1}), 343 nm (ε = 186.4 M^{-1} cm^{-1}) for **Yb2** and at 282 nm (ε = 11,449 M^{-1} cm^{-1}), 310.5 nm (ε = 1676 M^{-1} cm^{-1}) for **Yb3**.

The absorption spectra of a monocrystal of **Yb1** at 295 and 4 K are presented in Fig. 4. Those bands are assigned to the $^2F_{7/2} \rightarrow {}^2F_{5/2}$ transition of the Yb^{III} ion. At 295 K additional components corresponding to the transitions from thermally populated ligand-field levels of the ground state appear at wavelengths longer than 979.8 nm. The line at 979.8 nm is related to the lowest component of the $^2F_{5/2}$ (Fig. 4). The 4 K absorption spectrum consists of three main components corresponding to the $^2F_{7/2}(0) \rightarrow {}^2F_{5/2}(0', 1', 2')$ transitions. The ligand-field sublevels (Scheme 2) and total ligand-field splitting of $^2F_{5/2}$ state as 334 cm^{-1} (Fig. 4) were determined on the basis of the low temperature spectrum. Upon excitation in the ligand absorption band (270 nm), a relatively intense Yb^{III}-centered NIR emission is observed. The emission spectra at 295 and 4 K are also shown in Fig. 4. They display a band centered about 990 nm corresponding to $^2F_{5/2} \rightarrow {}^2F_{7/2}$ transition of the Yb^{III} ion. The spectrum at 4 K consists of four main components at 10,194, 10,074, 9901 and 9782 cm^{-1}. They arise from the M_J splitting of

Table 2
Selected bond lengths (Å) and angles (°) for **Er2** and **Yb3**.

Er2		**Yb3**	
Er–O52	2.258(2)	Yb–O52	2.257(3)
Er–O53	2.268(2)	Yb–O53	2.230(3)
Er–O54	2.278(2)	Yb–O54	2.244(3)
Er–O12	2.339(2)	Yb–O12	2.358(3)
Er–O13	2.362(2)	Yb–O13	2.300(3)
Er–O14	2.446(2)	Yb–O14	2.407(3)
Er–N21	2.528(2)	Yb–N21	2.482(4)
Er–N11	2.544(2)	Yb–N11	2.563(4)
O52–Er–O53	108.86(7)	O53–Yb–O54	83.80(1)
O52–Er–O54	141.22(6)	O53–Yb–O52	113.63(1)
O53–Er–O54	90.36(7)	O54–Yb–O52	143.73(1)
O52–Er–O12	74.11(6)	O53–Yb–O13	75.98(1)
O53–Er–O12	77.33(7)	O54–Yb–O13	79.51(1)
O54–Er–O12	144.33(6)	O52–Yb–O13	74.83(1)
O52–Er–O13	76.01(7)	O53–Yb–O12	75.19(1)
O53–Er–O13	74.66(7)	O54–Yb–O12	142.67(1)
O54–Er–O13	77.29(7)	O52–Yb–O12	73.58(1)
O12–Er–O13	129.11(6)	O13–Yb–O12	123.11(1)
O52–Er–O14	143.24(7)	O53–Yb–O14	76.86(1)
O53–Er–O14	77.21(7)	O54–Yb–O14	74.63(1)
O54–Er–O14	72.62(7)	O52–Yb–O14	138.49(1)
O12–Er–O14	72.04(6)	O13–Yb–O14	144.10(1)
O13–Er–O14	138.22(6)	O12–Yb–O14	70.78(1)

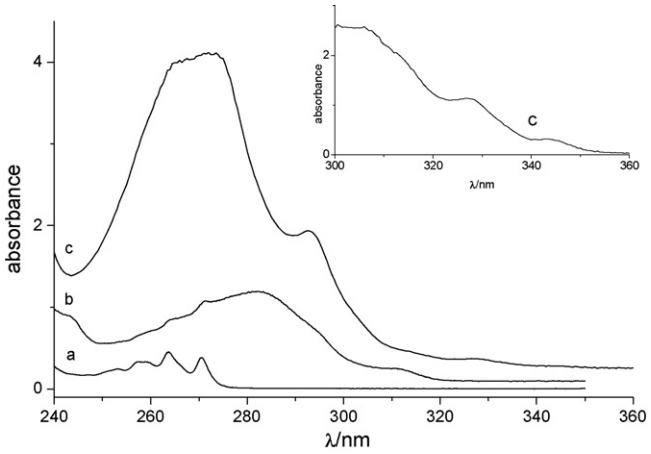

Fig. 3. The absorption spectra of **Yb1** (a), **Yb3** (b) and **Yb2** (c) in CH_3OH at 295 K, $c = 1.77 \times 10^{-3}$ M, $l = 0.1$ cm. The inset shows the absorption spectrum of **Yb2** (c) for $l = 1$ cm.

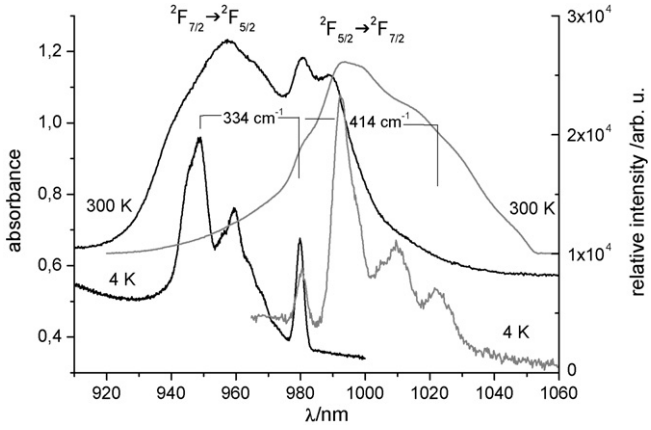

Fig. 4. The luminescence (λ_{exc} = 266 nm – xenon lamp) and absorption spectra of **Yb1** at 295 and 4 K.

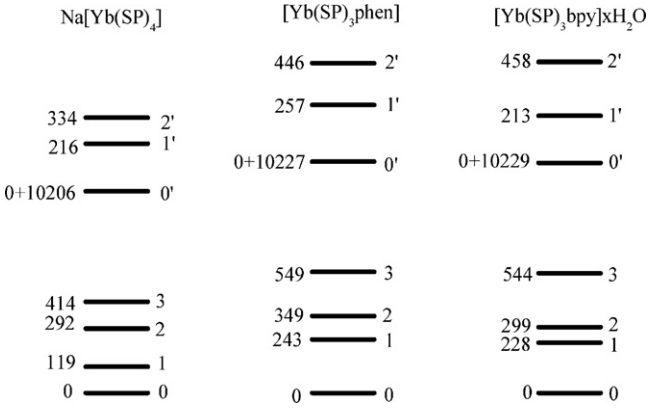

Scheme 2. The crystal field splitting of Yb^{III} levels for different complexes.

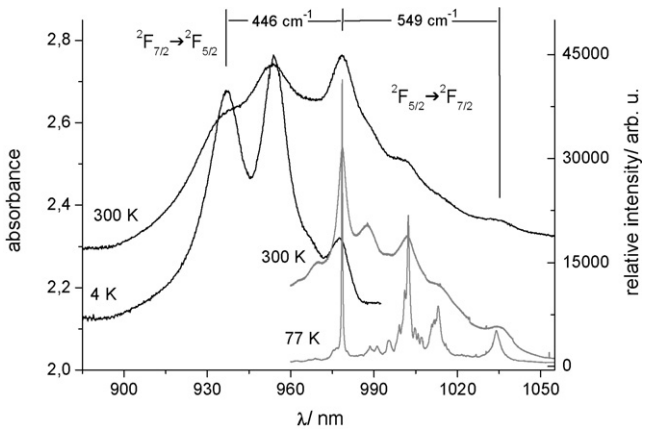

Fig. 5. The luminescence (λ_{exc} = 266 nm) and absorption spectra of **Yb2** at 295, 77 and 4 K.

$^2F_{7/2}$ state as the consequence of ligand-field effects. On the basis of 4 K emission spectrum, the ligand-field sublevels (Scheme 2) and total ligand-field splitting of $^2F_{7/2}$ state as 414 cm^{-1} (Fig. 4) were determined.

The absorption and emission spectra at different temperatures of **Yb2** and **Yb3** in solid state are presented in Figs. 5 and 6, respectively. The room temperature spectra display bands correspond to the $^2F_{7/2} \rightarrow {}^2F_{5/2}$ transition. The bands consist of three strong board peaks, centered at about 960 nm, accompanied by four broad wings in the lower energy region (>978 nm). They have much lower intensity because they represent the transitions from thermally populated ligand-field levels of the ground state. Three of those four weak absorption bands overlap the electronic lines of the $^2F_{5/2}(0') \rightarrow {}^2F_{7/2}(1, 2, 3)$ transitions in the 77 K emission spectra. In the 4 K absorption spectra, all of the broad wings disappear.

The ligand-field splitting of the excited ($^2F_{5/2}$) and ground ($^2F_{7/2}$) states determined as 446 and 549 cm^{-1}, and 458 cm^{-1} and 544 cm^{-1} respectively for **Yb2** and **Yb3** are indicated by brackets in Figs. 5 and 6. Ligand-field sublevels of Yb^{III} for **Yb2** and **Yb3**, determined from low temperature emission and absorption spectra, are presented in Scheme 2. The lines at 977.8 nm for **Yb2** and 977.6 nm for **Yb3** correspond to the lowest component of the $^2F_{5/2}$ state, since at those wavelengths the absorption and emission lines overlap at low temperature.

The emission spectra at both temperatures recorded by exciting the ligand excited level display bands assigned to the $^2F_{5/2} \rightarrow {}^2F_{7/2}$ transitions of the Yb^{III} ion. The room temperature emission spectra consist of five bands located in the lower energy region from the most intensive ones, $^2F_{5/2}(0') \rightarrow {}^2F_{7/2}$ (0). They are accompanied by broad wings located in the higher energy region exhibiting low intensity because they represent the transitions from thermally populated ligand-field sublevels of the excited state. The bands located in the 983.5–992.5 nm spectral range have the same origin and are of the e(2′–3) and e(1′–2) type for **Yb2** and **Yb3**. The reabsorption phenomenon for the investigated complexes is much lower then for inorganic compounds of Yb^{III} [23], where the $^2F_{5/2}(0') \rightarrow {}^2F_{7/2}(0)$ transition has very low intensity or is undetectable. This is because of the longer Yb–Yb distances in the organic complexes with large ligands in the former. The electronic emission lines e(0′–0), e(0′–1), e(0′–2), e(0′–3) are accompanied by a large number of weaker lines of mostly vibronic origin and thermally populated Stark sublevels. It is know that for Yb^{III} occur strong electron–phonon mixes of both electronic and vibronic transitions.

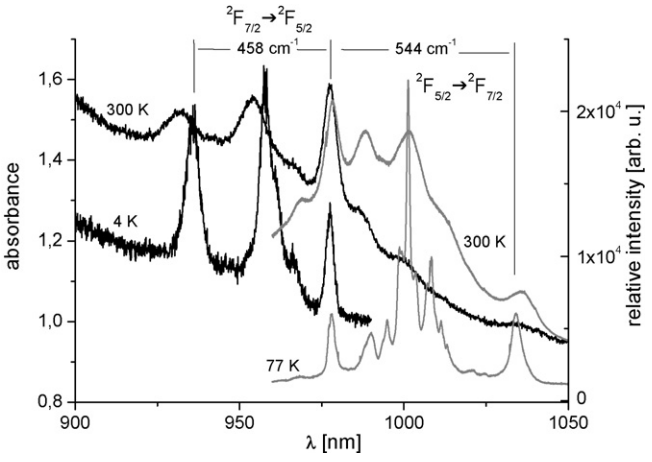

Fig. 6. The luminescence (λ_{exc} = 266 nm) and absorption spectra of **Yb3** at 295, 77 and 4 K.

Total ligand-field splitting of the excited and ground states of **Yb2** and **Yb3** is very similar. This is due to low point symmetry of Yb^{III} and the similar crystal structure of both complexes that differ only in the co-ligand molecule (phen or bpy). The splitting of the $^2F_{7/2}$ and $^2F_{5/2}$ states is much larger than for monocrystal of $Na_3[Yb(dpa)_3]\cdot 13H_2O$ (348 and 268 cm^{-1}) reported by Reinhard and Güdel [17], where site symmetry of Yb^{III} is D_2- and Yb(III) is D_3-symmetrical helicates (372 and 269 cm^{-1}), reported by Bünzli and co-workers [16]. In contrast, for a Yb^{III} complex in a low symmetry, a value of splitting of the $^2F_{7/2}$ of 528 cm^{-1} has been found and 455 cm^{-1} for another type of complexes [11]. In accordance with the above, higher site symmetry of Yb^{III} of **Yb1** (close D_{2d} [41]) results in the smaller total ligand-field splitting of the $^2F_{7/2}$ and $^2F_{5/2}$ states, as compared to **Yb2** and **Yb3** with site symmetry close C_{2v}.

All three investigated complexes exhibit sensitized luminescence of Yb^{III} at the temperature range from 300 to 4 K. The facts that the Yb^{III} emission (λ_{exc} = 266 nm) at room and 77 K was easily recordable for all the complexes using a 400 W xenon lamp as an excitation source, which is known to have a very low emission intensity at the UV range and the excitation was into tail of band with small molar absorption coefficient (see excitation (Fig. 8) and absorption spectra (Fig. 3)) in the lack of phosphorescence prove relatively efficient ligand-to-metal energy transfer. An additional element unfavourable to the excitation with the 266 nm wavelength is an energy gap between the triplet excited state of the [**SP**]$^-$ ligand and the $^2F_{5/2}$ excited level of the Yb^{III} ion, which is 15,335 cm^{-1} for the complex **Yb1**. Consequently, the exchange or dipol–dipol mechanism cannot be accepted. In spite of such a large energy gap, it is possible to observe the effective energy transfer from the ligand to the metal ion. At 77 K the ligand phosphorescence is not recordable for all three types of complexes. There are discussions in literature regarding the mechanism of the energy transfer at such a large energy gap. It is explained based on electron transfer involving the Yb^{III}/Yb^{II} redox process [26] or involving a simple SCC model, where the whole $Na_3[Yb(dpa)_3]\cdot 13H_2O$ complex is considered as a chromophore [17].

The lowest position of the triplet state of the [**SP**]$^-$ ligand (25,920 cm^{-1}) was determined on the basis of the phosphorescence spectrum of the **Gd1** complex in the solid state at 77 K. The lowest position of triplet states in complexes **Yb2** and **Yb3** was also determined from the phosphorescence spectra of **Lu2** and **Lu3** and they are 22,222 cm^{-1} and 23,310 cm^{-1} accordingly, and energy gaps $\Delta E = E_{trip} - E_{2F_{5/2}}$ are 11,550 and 12,620 cm^{-1}. Fig. 7 shows the phosphorescence spectra of **Gd1**, **Lu2** and **Lu3**. In complexes **Ln2** and **Ln3**, one molecule of the [**SP**]$^-$ ligand was replaced by the phen and bpy molecule, respectively. Excited singlet and triplet states of those co-ligands are lying at the lower energies as compared to the energy levels of the [**SP**]$^-$ ligand, and it seems that those lower-

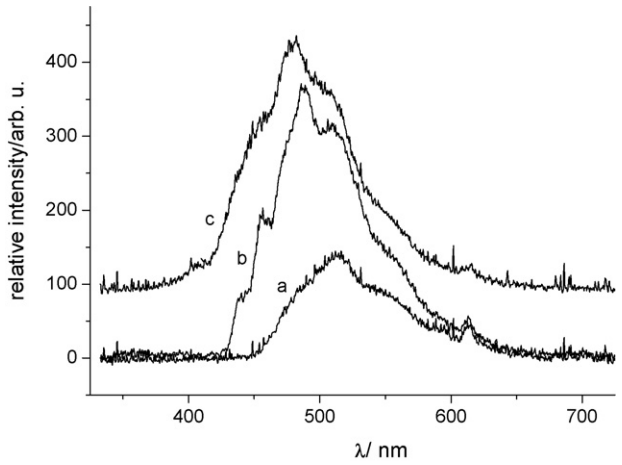

Fig. 7. The phosphorescence (λ_{exc} = 266 nm) spectra of **Lu2** (a), **Lu3** (b) and **Gd1** (c) at 77 K.

Table 3
The emission decay times of $^2F_{5/2}$ level and intrinsic quantum yield for **Yb1**, **Yb2**, **Yb3** (λ_{exc} = 266 nm). The decay time values were estimated with error of 10%.

	τ (μs)		Q_{Ln}^{Ln} (%)
	295 K	77 K	295 K
Yb1	35	40	3.14
Yb2	20	18	2.19
Yb3	15.5	16.5	1.64

lying levels would make it easier to transfer energy from a ligands to the Yb^{III} ion. However, it turned out that the introduction of those co-ligands did not improve the intensity of sensitized emission of the Yb^{III} ion.

Replacing one molecule of the $[\mathbf{SP}]^-$ ligand with the phen or bpy molecule caused reduction in the emission decay time at 295 K from 35 μs for the complex **Yb1** to 20 and 15.5 μs for the complexes **Yb2** and **Yb3**, respectively. Emission decay times for three studied complexes in the solid state at the temperature of 295 and 77 K are presented in Table 3. All curves of emission decay, presented in Fig. 8, can be fitted with a monoexponential function, which indicates the presence of only one emitting centre. No significant differences in the values of emission decay times were observed, when temperature was lowered (Table 3). Important factor which reduces the decay time and the intrinsic emission quantum yield (Q_{Ln}^{Ln}) for **Yb2** and **Yb3** as a result of introduction of co-ligand is increased contribution of multiphonon process of emission quenching. In the quenching mechanism the high

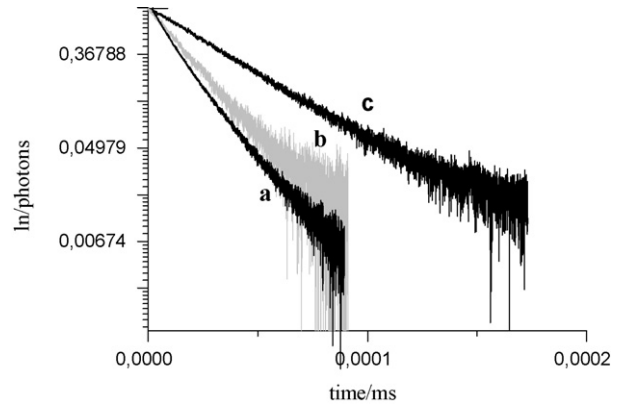

Fig. 8. The luminescence decays of **Yb3** (a), **Yb2** (b) and **Yb1** (c) at 295 K (λ_{exc} = 266 nm).

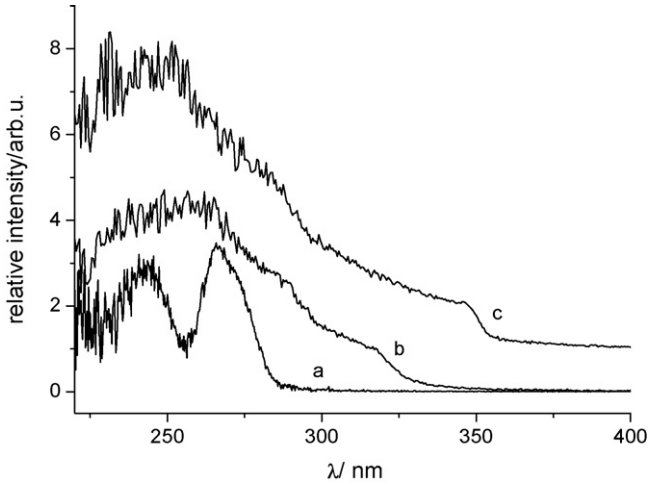

Fig. 9. The excitation spectra of (a) **Yb1** (λ_{mon} = 992 nm), (b) **Yb3** (λ_{mon} = 1001 nm), and (c) **Yb2** (λ_{mon} = 1035 nm) at 77 K.

energetic C–H vibration stretching (≈3000 cm^{-1}) and deformating (≈1600 cm^{-1}) of heteroaromatic rings are involved. Moreover, the presence of the one water molecule in the outer coordination sphere of **Yb3** is an additional factor of the emission quenching. It is reflected in shortening of the decay time for **Yb3** as related to **Yb2**. The intrinsic emission quantum yields (Q_{Ln}^{Ln}) were calculated from lifetimes:

$$Q_{Ln}^{Ln} = \frac{\tau_{obs}}{\tau_{rad}}$$

where τ_{obs} is the observed decay time of the emitting excited state and τ_{rad} the radiative lifetime of this state. τ_{rad} was estimated from the integrated absorption spectrum with a modified Einstein equation [42]:

$$\frac{1}{\tau_{rad}} = 2303 \times \frac{8\pi c n^2 \tilde{\nu}^2 (2J+1)}{N_A (2J+1)} \int \varepsilon(\tilde{\nu}) d\tilde{\nu}$$

where c is the speed of light in cm s^{-1}, N_A is Avogadro's number, J and J' are the quantum number's for the ground and excited states, respectively, $\int \varepsilon(\tilde{\nu}) d\tilde{\nu}$ is the integrated spectrum of the f–f transition, $\tilde{\nu}$ is the barycentre of the transition and n is the refractive index. The following results of the intrinsic quantum yields were obtained: 3,18% (τ_{rad} = 1.12 ms, $\tilde{\nu}$ = 10242 cm^{-1}, n = 1.527), 1.64% (τ_{rad} = 943 μs, $\tilde{\nu}$ = 10386 cm^{-1}, n = 1.510) and 1.72% (τ_{rad} = 901 μs, $\tilde{\nu}$ = 10362 cm^{-1}, n = 1.537) for **Yb1**, **Yb2** and **Yb3**, respectively. Molar absorption coefficients (ε) for complexes are equal 2.35 M^{-1} cm^{-1} (10,198 cm^{-1}), 3.30 M^{-1} cm^{-1} (10,221 cm^{-1}), 3.35 M^{-1} cm^{-1} (10,220 cm^{-1}) for **Yb1**, **Yb2** and **Yb3** respectively. The $^2F_{5/2}$ excited state decay time of **Yb1** is one of the longest known for Yb(III) complexes in the solid state, for example, some of the longest are reported as follows: 14.1 μs [43], 17.8 μs [44], 20.6 μs [22], 22.6 μs [45]. According to literature reports, the values from several to about dozen of μs were determined for majority of Yb^{III} complexes in the solid state, as well as the intrinsic quantum yield is one of the greatest. Unprecedented long decay times for the Yb(III) fluorinated complex in solid state (582 μs) and in CD_3CN (1111 μs) have recently been found by Pikramenou and co-workers [46].

Excitation spectra of **Yb1**, **Yb2** and **Yb3** are shown in Fig. 9. Considering molar absorption coefficients excitation into lower-lying bands of phen and bpy is more effective than excitation into their higher-lying bands (λ_{max} = 272 nm—**Yb2**; λ_{max} = 282 nm—**Yb3**). The proof of this is the presence of phen and bpy bands in the excitation spectra of **Yb2** and **Yb3** where their molar absorption coefficients are approximately about 120 (λ = 343 nm) and 7 (λ = 310.5 nm)

times smaller than for λ = 272 and λ = 282 nm respectively. It has to be associated with a mechanism of energy transfer from the ligand to the metal ion, where the excitation of the Yb^{III} ion may occur through a double electron transfer [26] in addition to a common phonon-assisted transfer mechanism [17].

Phen and bpy are more electron-withdrawing than $[\mathbf{SP}]^-$ so substitution of one of the $[\mathbf{SP}]^-$ ligands with phen or bpy affects the redox behavior, which should cause the change of the luminescence properties if the main factor of energy transfer occur through a double electron transfer. However, phen and bpy co-ligands have also the absorption bands in the same spectral region (240–280 nm) as $[\mathbf{SP}]^-$ ligand. This overlapping makes the comparison of excitation effectiveness through the $[\mathbf{SP}]^-$ ligand impossible even if the sensitization efficiency (η_{sens}) is known. Due to insufficient amount of monocrystals of the complexes the Q^{L}_{LN} was impossible to be determined. Therefore η_{sens} for the given complexes has not been estimated yet. These parameters shall be determined and included in the upcoming manuscript in which the next complexes with sulfonyl phosphoramide derivative—dimethyl(phenylsulfonyl)amidophosphate will be investigated.

The emission of Er^{III} in **Er1**, **Er2** and **Er3** single crystals was not detectable using our experimental set-up.

4. Conclusions

The complexes which exhibit relatively both efficient ligand-to-metal energy transfer and strong metal-centred emission are worth investigation with the perspective of creation more effective energy converters. In this context the new series of the Yb^{III} complexes under investigation seems to be promising as a device converting UV light to infrared radiation.

For complexes **Ln1**, **Ln2** and **Ln3**, which are stable under exposure to UV laser radiation, and even synchrotron radiation, effective energy transfer from the ligand to the Yb^{III} ion was demonstrated. For **Yb1**, despite a large energy gap $\Delta E = E_{trip} - E_{2F_{5/2}}$ of 15,335 cm^{-1}, sensitized emission with one of the longest emission decay time of 35 μs (radiative lifetime of 1.12 ms and $Q^{Ln}_{Ln} = 3.18\%$) was detected. Ligand-to-metal energy transfer in **Yb1**, **Yb2** and **Yb3** is efficient because of the lack of ligand emission and possibility of excitation of the metal-centred emission using the xenon lamp UV radiation.

Replacing one molecule of the $[\mathbf{SP}]^-$ ligand by phen or bpy molecule in **Yb2** and **Yb3** is disadvantageous because of Q^{Ln}_{Ln}. High energetic C–H vibrations of heteroaromatic rings of phen or bpy and O–H of one water molecule in **Yb3** complex result in increased contribution of multiphonon process in emission quenching. The decreasing of decay time and the intrinsic quantum yield of **Yb2** and **Yb3** is the result of the above. On the other hand such the replacing gives a possibility to excite the Yb^{III} emission at lower energy. According to the molar absorption coefficients the excitation of the Yb^{III} emission into the phen at 343 nm or bpy at 310 nm absorption bands is more effective than excitation into their absorption bands lying at higher energies.

Please note that it is impossible to estimate how the substitution of one $[\mathbf{SP}]^-$ molecule by the more electron-withdrawing co-ligands influence the efficiency of energy transfer from $[\mathbf{SP}]^-$ ligand to the metal ion, because some of the co-ligands absorption bands are located in the same spectral region (240–280 nm) as those of $[\mathbf{SP}]^-$ ligand.

Moreover, this article demonstrates that the use of high-resolution emission and absorption spectroscopy at low temperatures makes it possible to determine the ligand-field splitting of the low-lying states in the Yb^{III} crystal complexes.

Acknowledgements

The authors would like to thank Dr. Lucjan Jerzykiewicz and Prof. Tadeusz Lis for helpful crystallographic discussion as well as to Msc Paweł Głuchowski for decay times measurements and wish to acknowledge the support through a Grant No. N N204 131838 from the Polish Committee for Scientific Research.

References

[1] S. Shionoya, W.M. Yen, Phosphor Handbook, CRC Press Inc., Boca Raton, FL, 33431, USA, 1999.
[2] J.-C.G. Bünzli, C. Piguet, Chem. Soc. Rev. 34 (2005) 1048.
[3] J. Kido, Y. Okamoto, Chem. Rev. 102 (2002) 2357.
[4] S. Faulkner, J.L. Matthews, in: M.D. Ward (Ed.), Comprehense Coordination Chemistry II, vol. 9, Elsevier Pergamon, Amsterdam, 2004, pp. 913–944 (Chapter 9.21).
[5] S. Faulkner, S.J.A. Pope, B.P. Burton-Pye, Appl. Spectrosc. Rev. 40 (2005) 1.
[6] J.W. Stouwdam, F.C.J.M. Van Veggel, Nano Lett. 2 (2002) 733.
[7] P. Salvadori, C. Rossini, C. Bertucci, J. Am. Chem. Soc. 106 (1984) 2439.
[8] M.H.V. Werts, R.H. Woudenberg, P.G. Emmerink, R. van Gassel, J.W. Hofstraat, J.W. Verhoeven, Angew. Chem., Int. Ed. 39 (2000) 4542.
[9] E.F. Gudgin Dickson, A. Pollak, E.P. Diamandis, J. Photochem. Photobiol. B 27 (1995) 3.
[10] A. Mayer, S. Neuenhofer, Angew. Chem., Int. Ed. Engl. 33 (1994) 1044.
[11] (a) S. Comby, J.-C.G. Bünzli, Lanthanide near-infrared luminescence in molecular probes and devices, in: Handbook on the Physics and Chemistry of Rare Earth, vol. 37, Elsevier Science B.V., Amsterdam, 2007 (Chapter 235);
(b) S.V. Eliseeva, J.-C.G. Bünzli, Chem. Soc. Rev. 39 (2010) 189.
[12] T. Lazarides, M.A.H. Alamiry, H. Adams, S.J.A. Pope, S. Faulkner, J.A. Weinstein, M.D. Ward, Dalton Trans. (2007) 1484–1491.
[13] N.M. Shaveleev, R. Scopelliti, F. Gumy, J.-C. Bünzli, Eur. J. Inorg. Chem. (2008) 1523–1529.
[14] J. Zhang, S. Petoud, Chem. Eur. J. 14 (2008) 1264–1272.
[15] A. Beeby, S. Faulkner, J.A.G. Williams, J. Chem. Soc., Dalton Trans. (2002) 1918–1922.
[16] F.R. Goncalves e Silva, O.L. Malta, Ch. Reinhard, H.-U. Güdel, C. Piguet, J.E. Moser, J.-C.G. Bünzli, J. Phys. Chem. A 106 (2002) 1670–1677.
[17] Ch. Reinhard, H.U. Güdel, Inorg. Chem. 41 (2002) 1048–1055.
[18] Y. Korovin, N. Rusakova, J. Fluoresc. 12 (2002) 159–161.
[19] S. Quici, M. Cavazzini, G. Marzanni, G. Accorsi, N. Armaroli, B. Ventura, F. Barigelletti, Inorg. Chem. 44 (2005) 529–537.
[20] S. Comby, D. Imbert, A.S. Chauvin, J.-C.G. Bünzli, Inorg. Chem. 45 (2006) 732–743.
[21] S. Comby, D. Imbert, C. Vandevyver, J.-C.G. Bünzli, Chem. Eur. J. 13 (2007) 936–944.
[22] M. Albrecht, O. Ostecka, J. Klankermayer, R. Fröhlich, F. Gumy, J.-C.G. Bünzli, Chem. Commun. (2007) 1834–1836.
[23] G. Boulon, J. Alloys Compd. 451 (2008) 1–11.
[24] J. Legendziewicz, J. Cybinska, M. Guzik, G. Boulon, G. Meyer, Opt. Mater. 30 (2008) 1655–1666.
[25] J. Legendziewicz, J. Sokolnicki, J. Alloys Compd. 451 (2008) 600.
[26] W.D. Horrocks Jr., J.P. Bolender, W.D. Smith, R. Supkowski, J. Am. Chem. Soc. 119 (1997) 5972–5973.
[27] (a) P. Gawryszewska, J. Sokolnicki, J. Legendziewicz, Coord. Chem. Rev. 249 (2005) 2489;
(b) P. Gawryszewska, J. Sokolnicki, A. Dossing, J.P. Riehl, G. Muller, J. Legendziewicz, J. Phys. Chem. A 109 (2005) 3858;
(c) P. Gawryszewska, O.L. Malta, R. Longo, F.R.G.E. Silva, K. Mierzwicki, Z. Latajka, M. Pietraszkiewicz, J. Legendziewicz, Chem. Phys. Chem. 5 (2004) 1;
(d) P. Gawryszewska, Z. Ciunik, J. Photochem. Photobiol. A 202 (2009) 1–9.
[28] G.F. de Sá, O. Malta, C. de Mello Donega, A.M. Simas, R.L. Longo, P.A. Santa-Cruz, E.F. da Silva, Coord. Chem. Rev. 196 (2000) 165.
[29] S. Lis, M. Elbanowski, B. Mąkowska, Z. Hnatejko, J. Photochem. Photobiol. 150 (2002) 233–247.
[30] O.L. Malta, J. Non-Cryst. Solid 354 (2008) 4770–4776.
[31] L.R. Melby, N.J. Rose, E. Abramson, J.C. Caris, J. Am. Chem. Soc. 86 (1964) 5117.
[32] S.B. Meshkova, N.V. Rusakova, Z.M. Topilova, M.O. Lozinski, L.S. Kudryavtseva, Russ. J. Coord. Chem. (Engl. Transl.) 18 (1992) 183.
[33] (a) V. Tsaryuk, V. Zolin, J. Legendziewicz, Spectrochim. Acta A 54 (1998) 2247;
(b) V. Tsaryuk, J. Legendziewicz, L. Puntus, V. Zolin, J. Sokolnicki, J. Alloys Compd. 300–301 (2000) 464.
[34] A. Bellusci, G. Barberio, A. Crispini, M. Ghedini, M. La Deda, D. Pucci, Inorg. Chem. 44 (2005) 1818.
[35] O.V. Moroz, V.A. Trush, I.S. Konovalova, O.V. Shishkin, Y.S. Moroz, S. Demeshko, V.M. Amirkhanov, Polyhedron 28 (2009) 1331–1335.
[36] A.V. Kirsanov, Fosfazosoedineniya (Phosphazo Compounds), 16, Naukova Dumka, Kiev, 1965.
[37] O.V. Moroz, S.V. Shishkina, V.A. Trush, T.Yu. Sliva, V.M. Amirkhanov, Acta Crystallogr. E 63 (2007) m3175.
[38] G.M. Sheldrick, Acta Crystallogr. A 46 (1990) 467–473.
[39] G.M. Sheldrick, SHELXL97, Program for Crystal Structure Refinement, University of Göttingen, 1997.

[40] (a) S. Onuma, H. Inoue, S. Shibata, Bull. Chem. Soc. Jpn. 49 (1976) 644;
(b) J.H. Burns, M.D. Danford, Inorg. Chem. 8 (1969) 1780.
[41] D. Kulesza, M. Sobczyk, J. Legendziewicz, O. Moroz, V. Amirkhanov, Struct. Chem. 21 (2010) 425–438.
[42] M.H.V. Werts, R.T.F. Jukes, J.W. Verhoeven, Phys. Chem. Chem. Phys. 4 (2002) 1542.
[43] N.M. Shavaleev, S.J.A. Pope, Z.R. Bell, S. Faulkner, M.D. Ward, Dalton Trans. (2003) 808.
[44] A.P. Bassett, R.V. Deun, P. Nockemann, P.B. Glover, B.M. Kariuki, K.V. Hecke, L.V. Meervelt, Z. Pikramenou, Inorg. Chem. 44 (2005) 6140.
[45] M. Albrecht, R. Fröhlich, J.-C.G. Bünzli, A. Aebischer, F. Gumy, J. Hamacek, J. Am. Chem. Soc. 129 (2007) 14178.
[46] P.B. Gloger, A.P. Bassett, P. Nockemann, B.M. Kariuki, R.V. Deun, Z. Pikramenou, Chem. Eur. J. 13 (2007) 6308.